J. Phys. D: Appl. Phys. **31** (1998) 1817–1822. Printed in the UK PII: S0022-3727(98)89599-5

On asymptotic values of light fluxes scattered by large spherical particles between two angles

Alexander A Kokhanovsky†, Victor A Babenko‡ and Vladimir V Barun‡

† Institute of Particle Technology and Environmental Engineering, Technical University of Clausthal, Leibnizstrasse 19, D-38678 Clausthal-Zellerfeld, Germany
‡ Stepanov Institute of Physics, National Academy of Sciences of Belarus, 68 F Scarina Avenue, 220072 Minsk, Belarus

Received 28 November 1997, in final form 27 April 1998

Abstract. The asymptotical limits for light fluxes scattered by large spherical particles with various refractive indices into a fixed range of scattering angles are obtained. Calculations are performed within the framework of the Mie theory and the geometrical optics approximation. The geometrical optics approach, combined with approximations of the radiative transfer theory, allows one to make quick estimates of reflection and transmission functions of disperse media with large particles. The results obtained can be used for studies of light fields in random media with large particles within the framework of the small-angle and quasi-single-scattering approximations of the radiative transfer theory.

1. Introduction

The fluxes scattered by small particles between two angles are important parameters in various approximations of the radiative transfer theory. For instance, the reflection function R of strongly absorbing semi-infinite light-scattering layers with large particles can be calculated with the following equation [1]:

$$R(\eta, \eta_0, \phi) = \frac{\omega_0 p(\theta)}{4[1 - \omega_0 F(\pi/2)](\eta + \eta_0)} \qquad (1)$$

where ω_0 is the single-scattering albedo, defined as the ratio of scattering and extinction coefficients, $p(\theta)$ is the phase function with the normalization condition $\frac{1}{2}\int_0^\pi p(\theta)\sin\theta\,\mathrm{d}\theta = 1$, $\theta = \arccos\{-\eta\eta_0 + [(1-\eta^2)(1-\eta_0^2)]^{1/2}\cos\psi\}$ is the scattering angle, $\eta = \cos\vartheta$, $\eta_0 = \cos\vartheta_0$, ψ is the azimuth of the reflected radiation, ϑ is the angle of observation, ϑ_0 is the angle of incidence and $F(\pi/2) = \frac{1}{2}\int_0^{\pi/2} p(\theta)\sin\theta\,\mathrm{d}\theta$ is the light flux, scattered in the forward hemisphere. The flux scattered in the range of scattering angles smaller then $\theta = \pi/4$, $F(\pi/4) = \frac{1}{2}\int_0^{\pi/4} p(\theta)\sin\theta\,\mathrm{d}\theta$, is an important parameter of the small-angle approximation of the radiative transfer theory [1].

One can find values of ω_0 and $p(\theta)$ with the Mie theory and calculate the light flux $F(\theta_0)$ scattered between angles 0 and θ_0 afterwards. It is a well-known fact that the single-scattering albedo, the flux $F(\theta_0)$ and the phase function of the elementary volume of a light-scattering medium approach some asymptotic limits as the size of particles increases [2]. These asymptotical geometrical optics values for the single-scattering albedo, the extinction coefficient and the phase function have already been studied in numerous publications [2–5].

The task of this paper is to find geometrical optics (GO) asymptotic values for the fluxes $F(\pi/4)$, $F(\pi/2)$, $\phi(\pi/4) = 1 - F(\pi/4)$ and $\phi(\pi/2) = 1 - \phi(\pi/2)$. This is important both from the point of view of practical applications (see equation (1)) and on general grounds. These asymptotical limits differ for nonabsorbing and absorbing particles. Thus, we consider cases of absorbing and nonabsorbing particles with various refractive indices separately. Note that our results for strongly absorbing spherical particles can be applied for convex nonspherical particles at random orientation as well [2].

The computation of $F(\theta_0)$ for spherical particles or their polydispersions is usually performed with the Mie theory [2]. To this end two different approaches are used. In the framework of the first one the above quantities are calculated by the direct integration of the phase function, obtained with the Mie theory [2]. In addition to commonly known difficulties associated with the Mie theory computations for large particles, one frequently comes up against the solution of the problem due to the well-known ripple structure of the phase function for particles with low absorption. Thus, the second approach, namely the use of the double series [6–8] in the Mie scattering coefficients, is preferable in our opinion. We use this second approach to validate the geometrical optics calculations.

0022-3727/98/151817+06$19.50 © 1998 IOP Publishing Ltd

2. The geometrical optics approximation for calculating fluxes between two scattering angles

2.1. Basic equations

The radiation scattered by a particle can be divided into two parts (diffracted and geometrical optical components) in the framework of the GO approximation. Such a separation can be valid only for large, optically dense scatterers ($\rho \gg 1$, $L \gg 1$, where $\rho = ka$, $L = 2ka|m-1|$, a is the radius of a spherical particle, $m = n - \mathrm{i}\chi$ is the relative complex refractive index of particle's substance, $k = 2\pi/\lambda$, λ is the wavelength of the incident radiation). For the sake of simplicity we assume that $\chi \ll n$ and $n > 1$. This case holds good for a number of natural media in the optical range (water and dust clouds, soils, snow fields and so on).

In the framework of the ray optics approximation the phase function of a spherical particle with the radius a can be written as follows:

$$p(\theta) = [p^D(\theta)\sigma^D_{sca} + p^G(\theta)\sigma^G_{sca}]/(\sigma^D_{sca} + \sigma^G_{sca}). \tag{2}$$

Here σ^D_{sca} and σ^G_{sca} are the scattering cross sections, defined accordingly for processes of diffraction and GO scattering. The values of $p^D(\theta)$ and $p^G(\theta)$ are phase functions of the corresponding processes. The analytical expressions for all these quantities are well known [2–5]:

$$\sigma^D_{sca} = \pi a^2 \qquad \sigma^G_{sca} = w\pi a^2 \qquad p^D(\theta) = 4J_1^2(\theta\rho)/\theta^2$$

$$p^G(\theta) = \sum_{p=0}^{\infty} D(\theta)(\varepsilon_{1p} + \varepsilon_{2p})/w. \tag{3}$$

Here J_1 is the Bessel function $D(\theta) = \sin(2\tau)\,\mathrm{d}\tau/(\sin\theta\,\mathrm{d}\theta)$, τ is the angle of the incidence (following Debye [9], we define τ as the angle between the direction of the incident ray and the tangent to a particle surface), and

$$\varepsilon_{jp} = \delta_{0p}R_j(\tau) + (1 - R_j(\tau))^2(1 - \delta_{0p})R_j^{p-1}(\tau) \times \exp(-pc\xi) \tag{4}$$

$$w = \frac{1}{2}\sum_{j=1}^{2}\int_0^{\pi/2}\left(R_j(\tau) + \frac{(1 - R_j(\tau))^2\exp(-c\xi)}{1 - R_j(\tau)\exp(-c\xi)}\right) \times \sin(2\tau)\,\mathrm{d}\tau \tag{5}$$

$$R_1(\tau) = \left|\frac{\tan(\tau - \tau')}{\tan(\tau + \tau')}\right|^2 \qquad R_2(\tau) = \left|\frac{\sin(\tau - \tau')}{\sin(\tau + \tau')}\right|^2$$
$$\tau' = \arccos(\cos\tau/n) \tag{6}$$

where δ_{0p} is the Kronecker symbol, $c = 4\chi\rho$, $\xi = (1 - \cos^2\tau')^{1/2}$ and the scattering angle is related to τ by the following formula [2]:

$$\theta = 2\pi j + 2(-1)^k(\tau - p\tau') \tag{7}$$

where the integers j and k are chosen from the condition $\theta \in [0, \pi]$.

Thus, one can obtain the following equation for light fluxes scattered by a spherical particle in the cone with the apex θ_0 (see equation (2)):

$$F(\theta_0) = [F^D(\theta_0)\sigma^D_{sca} + F^G(\theta_0)\sigma^G_{sca}]/(\sigma^D_{sca} + \sigma^G_{sca}) \tag{8}$$

where

$$F^D(\theta_0) = 2\int_0^{\theta_0}[J_1^2(\theta\rho)/\theta^2]\sin\theta\,\mathrm{d}\theta \tag{9}$$

$$F^G(\theta_0) = \frac{1}{w}\sum_{p=0}^{\infty}A_p(\theta_0) \tag{10}$$

$$A_p(\theta_0) = \frac{1}{2}\int_{\tau_p^*}^{\tilde{\tau}_p}(\varepsilon_{1p} + \varepsilon_{2p})\sin(2\tau)\,\mathrm{d}\tau. \tag{11}$$

The values of angles τ_p^* and $\tilde{\tau}_p$ in equation (11) are specified from the condition that scattering beams with angles of incidence in the range $[\tau_p^*, \tilde{\tau}_p]$ fall within the interval of scattering angles $\theta \in [0, \theta_0]$.

Let us consider the integral (9). The integrand has a sharp peak near the scattering angle $\theta = 0$. Thus, instead of equation (9) one obtains ($\sin\theta \approx \theta$):

$$F^D(\theta_0) = 2\int_0^{\theta_0\rho}[J_1^2(y)/y]\,\mathrm{d}y. \tag{12}$$

This integral can be calculated analytically:

$$F^D(\theta_0) = 1 - J_0^2(\theta_0\rho) - J_1^2(\theta_0\rho). \tag{13}$$

Note that, for large values of θ_0 ($\theta_0 \gg 1/\rho$), it follows that

$$F^D(\theta_0) \approx 1. \tag{14}$$

The calculation of the integrals $A_p(\theta_0)$ is more difficult. It involves two steps. In the first step one should define the values of τ_p^* and $\tilde{\tau}_p$ and in the second one the values of $A_p(\theta_0)$ should be calculated (numerically, as a rule).

2.2. Absorbing particles

Equations (8), (10), (11) and (13) can be applied for particles with any values of the absorption parameter c. For strongly absorbing particles ($c \gg 1$) reflected rays vanish due to the high absorption of radiation inside scatterers. Thus, scattered light fluxes are determined by the reflection of rays from the surface of a particle only. The scattering angle θ is equal to 2τ (see equation (7)) for these rays ($p = 0$). Thus, one obtains that $\tau_0^* = 0$ and $\tilde{\tau}_0 = \theta_0/2$ in equation (11).

The integral

$$A_0(\theta_0) = \frac{1}{2}\int_0^{\theta_0/2}[R_1(\tau) + R_2(\tau)]\sin(2\tau)\,\mathrm{d}\tau \tag{15}$$

which follows from equation (11) at $p = 0$, can be calculated analytically:

$$A_0(\theta_0) = (n^2 - 1)^{-2}\{\tfrac{4}{3}z^3(z^3 - \nu^3) + 2\mu^2z^4 + \gamma^2\beta^2z^2 - 2n^2\beta\gamma^2\nu z - 4n^6\mu^2\gamma^2z(n^2z + \nu)^{-1} + 8n^4\beta\gamma^3 \times \ln[(n^2z + \nu)/\mu] - 2n^2(n^8 + 6n^4 + 1)\gamma^3 \times \ln[(z + \nu)/\mu]\} \tag{16}$$

where $z = \sin(\theta_0/2)$, $\beta = n^4 + 1$, $\gamma = (n^2 + 1)^{-1}$, $\nu = (z^2 + n^2 - 1)^{1/2}$ and $\mu = (n^2 - 1)^{1/2}$.

Thus, equation (16) can be used for calculations of asymptotical values of fluxes scattered by large strongly absorbing particles in the range of scattering angles $\theta \in [0, \theta_0]$. It is a well-known fact [2] that the scattering pattern caused by reflection of light from very large convex particles with random orientations is identical to the scattering pattern arising from reflection from a very

large sphere of the same material and surface conditions. Thus, equation (16) can be applied for convex nonspherical particles as well. For such particles, it follows that [2]

$$\omega_0 = 0.5(1 + A_0(\pi))$$

$$p^G(\theta) = \frac{1}{2A_0(\pi)}[R_1(\theta/2) + R_2(\theta/2)].$$

These formulae allow the simple calculation of reflection functions of turbid layers (see equations (1), (8) and (16) as well) with strongly absorbing particles. They can be used as a base for the extension of the ellipsometry of homogeneous layers in the case of disperse media [10]. Surfaces of randomly oriented particles in this case play the role of a plane surface, reflection from which is used for determination of the refractive index.

2.3. Nonabsorbing particles

For nonabsorbing particles one should consider not only reflected but also refracted rays. For instance, for the doubly refracted ray ($p = 1$) the scattering angle θ is related to the refraction angle τ' by the following formula (see equation (7)):

$$\theta = 2(\tau' - \tau) \tag{17}$$

where $\tau' = \arccos(\cos\tau/n)$. Thus, unlike the case discussed above ($p = 0$), the deflection angle for the ray with $p = 1$ depends not only on τ but also on the particle's refractive index [2–4]. It is evident that the scattering angle θ for the doubly refracted ray can be varied between 0 (at the central incidence, $\tau = \tau' = \pi/2$) and the value (see equation (17) at $\tau = 0$)

$$\theta_c = 2\arccos(n^{-1}). \tag{18}$$

For instance, it follows that $\theta_c \approx 82.8^\circ$ for water ($n = 1.33$) droplets in the visible. Thus, in this case all rays with $p = 1$ are concentrated in the forward hemisphere. They begin to come into the backward hemisphere at $n > \sqrt{2}$ only, as follows from equation (18).

Let us now consider the limits of integration τ_1^* and $\tilde{\tau}_1$ in equation (11). The limit $\tilde{\tau}_1$ is the solution of the following equation:

$$2[\arccos(\cos\tilde{\tau}_1/n) - \tilde{\tau}_1] = 0 \tag{19}$$

resulting from equation (17). It can be rewritten as

$$(n - 1)\cos\tilde{\tau}_1 = 0. \tag{20}$$

Therefore, it follows that $\tilde{\tau}_1 = \pi/2$ for $n \neq 1$. The limit τ_1^* is the solution of the following equation (see equation (17)):

$$2[\arccos(\cos\tau_1^*/n) - \tau_1^*] = \theta_0. \tag{21}$$

Equation (21) allows one to obtain the analytical solution

$$\tau_1^* = \arcsin[(1 - \Delta)/(1 + n^2 - 2\Delta)^{1/2}] \tag{22}$$

where

$$\Delta = n\cos(\theta_0/2). \tag{23}$$

Thus, it follows from equation (12) that

$$A_1(\theta_0) = \tfrac{1}{2}\int_{\tau_1^*}^{\pi/2}[(1 - R_1(\tau))^2 + (1 - R_2(\tau))^2] \times \exp(-c\xi)\sin(2\tau)\,d\tau \tag{24}$$

where τ_1^* is determined by equation (22).

The value of $A_1(\theta_0)$ rapidly decreases with increasing absorption parameter c and with decreasing refractive index n. Actually, one obtains that $A_1(\theta_0) \ll A_0(\theta_0)$ even at $c > 3$–5. This is true for $A_p(\theta_0)$ at $p > 1$ as well.

Thus, the contribution of terms with $p \geq 1$ in the sum $F^G(\theta_0)$ (see equation (10)) can be significant only for low-absorbing and transparent scatters having sufficiently large refractive indices.

It follows from equation (24) for nonabsorbing particles ($c = 0$) that

$$A_1(\theta_0) = \frac{1}{2}\int_{\tau_1^*}^{\pi/2}[(1 - R_1(\tau))^2 + (1 - R_2(\tau))^2]\sin(2\tau)\,d\tau. \tag{25}$$

In a similar way one can consider integrals $A_p(\theta_0)$ at $p \geq 2$. It will not be discussed in any details here.

3. Results of computations

3.1. Strongly absorbing and transparent scatterers

Let us apply now the derived solutions (8), (10), (11), (14), (16) and (25) to the computation of the asymptotical values of the backward flux $\phi(\pi/2) = 1 - F(\pi/2)$, the flux $\phi(\pi/4) = 1 - F(\pi/4)$ into the scattering angle range $\theta > \pi/4$ and the forwards–backwards ratio $\eta = F(\pi/2)/[1 - F(\pi/2)]$. Note that values of $\phi(\pi/2)$ and $\phi(\pi/4)$ are small for large particles. Thus, the forwards–backwards ratio is large.

We will consider two limiting cases here: strongly absorbing particles ($c \to \infty$, $\phi_\infty(\pi/4)$, $\phi_\infty(\pi/2)$, η_∞) and transparent spheres ($c = 0$, $\phi_0(\pi/4)$, $\phi_0(\pi/2)$, η_0), that approximately describe dust ($c \to \infty$) and cloud ($c = 0$) particles in the visible spectral range. In the first case, from equations (8) and (14) it follows that

$$\phi_\infty(\pi/4) = 1 - [1 + A_0(\pi/4)]/[1 + A_0(\pi)] \tag{26}$$

$$\phi_\infty(\pi/2) = 1 - [1 + A_0(\pi/2)]/[1 + A_0(\pi)] \tag{27}$$

$$\eta_\infty = (1 - \phi_\infty(\pi/2))/\phi_\infty(\pi/2) \tag{28}$$

where the values of $A_0(\pi/2)$, $A_0(\pi/4)$ and $A_0(\pi)$ are determined by equation (16).

The results of computation of asymptotical values $\phi_\infty(\pi/4)$ and $\phi_\infty(\pi/2)$ and the value of η_∞ with equations (16) and (26)–(28) for various values of the refractive index n are presented in table 1. In addition, figure 1 gives the comparison of results for $\phi_\infty(\pi/2)$ computed with equation (27) and the Mie theory. It follows from figure 1 that the error of the approximate expression (27) is less than 5% at $\rho = 10^3$, $n < 2$ and $\chi = 10^{-2}$. The accuracy of the GO results increases with increasing diffraction parameter ρ. As we mentioned before, our results (26)–(28) are valid for convex strongly absorbing

Table 1. Asymptotic fluxes scattered between two angles.

n	$\phi_0(\pi/2)$	$\phi_\infty(\pi/2)$	$\phi_0(\pi/4)$	$\phi_\infty(\pi/4)$	η_0	η_∞
1.05	0.0056	0.0004	0.0062	0.0016	177.8	2855.0
1.10	0.0104	0.0013	0.0124	0.0051	95.41	774.0
1.15	0.0149	0.0027	0.0211	0.0093	66.31	310.4
1.20	0.0192	0.0045	0.0359	0.0140	51.08	223.1
1.25	0.0235	0.0065	0.0554	0.0189	41.62	152.2
1.30	0.0277	0.0088	0.0775	0.0240	35.14	112.3
1.33	0.0302	0.0103	0.0913	0.0271	32.14	96.12
1.40	0.0359	0.0140	0.1234	0.0344	26.84	70.71
1.45	0.0363	0.0167	0.1451	0.0397	26.56	58.89
1.50	0.0401	0.0195	0.1656	0.0450	23.94	50.19
1.53	0.0424	0.0213	0.1772	0.0481	22.56	46.01
1.60	0.0483	0.0254	0.2020	0.0554	19.71	38.38
1.65	0.0528	0.0284	0.2181	0.0606	17.93	34.24
1.70	0.0577	0.0314	0.2327	0.0657	16.34	30.87
1.75	0.0628	0.0344	0.2461	0.0708	14.93	28.08
1.80	0.0681	0.0374	0.2584	0.0758	13.68	25.75
1.85	0.0736	0.0404	0.2696	0.0807	12.58	23.77
1.90	0.0793	0.0433	0.2799	0.0856	11.62	22.07
1.95	0.0850	0.0463	0.2894	0.0904	10.77	20.60
2.00	0.0907	0.0492	0.2981	0.0951	10.02	19.33

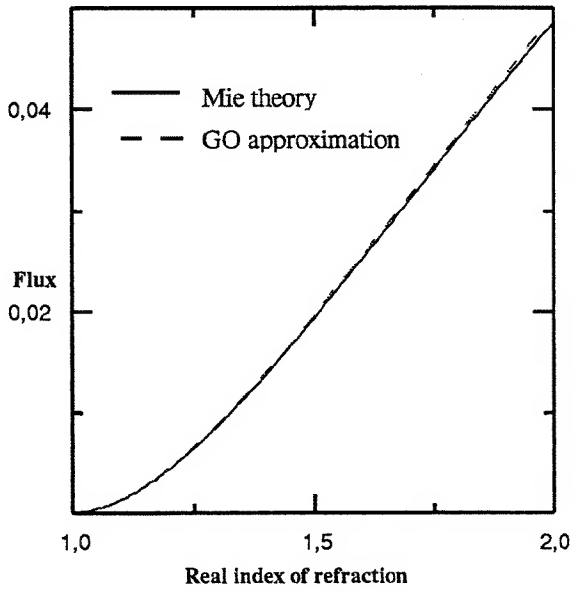

Figure 1. The flux $\phi_\infty(\pi/2)$ versus the particle's refractive index n (the full line shows the results of the Mie theory at $\chi = 10^{-2}$ and $\rho = 10^3$; the broken line is the calculation with equations (16) and (27)).

nonspherical particles at random orientations as well. This is an important point.

Let us consider now nonabsorbing ($c = 0$) large spherical particles. In this case one can obtain after simple calculations

$$\phi_0(\pi/4) = 1 - \frac{1}{2}\left(1 + \sum_{p=0}^{\infty} A_p(\pi/4)\right) \tag{29}$$

$$\phi_0(\pi/2) = 1 - \frac{1}{2}\left(1 + \sum_{p=0}^{\infty} A_p(\pi/2)\right) \tag{30}$$

$$\eta_\infty = (1 - \phi_0(\pi/2))/\phi_0(\pi/2). \tag{31}$$

The values of $A_p(\pi/4)$ and $A_p(\pi/2)$ were calculated numerically using equation (11) with $c = 0$. Note that we neglected the contribution of low-energy rays with $p > 3$ in order to simplify the computations. The obtained values of $\phi_0(\pi/4)$, $\phi_0(\pi/2)$ and η_0 are presented in table 1. As expected, the fraction of radiation scattered in the backward hemisphere for transparent ($c = 0$) particles is considerably larger than that for strongly absorbing ($c \to \infty$) ones. This fraction increases with increasing refractive index of the particle. It varies from 0.56% at $n = 1.05$ to 9.07% at $n = 2.0$. For example, only 3% of the incident energy is scattered in the backward hemisphere for large water drops.

The comparison of values $\phi_0(\pi/2)$ computed by the GO approximation and the Mie theory (with the use of the algorithm in [6]) is given in figure 2. The error of the GO approach (see equation (30)) is less than 10% at $n < 1.9$, $\rho = 1000$ and $c = 0$. It decreases with increasing diffraction parameter. Thus, the asymptotic GO limits for nonabsorbing particles are reached at larger sizes of particles than they are in the case of strongly absorbing scatterers.

The ripple structure on the Mie curve at $n \approx 2.0$ (see figure 2) can be explained by considering the interference of geometrical optics rays. It is evident that the polydispersity of a medium will totally suppress this structure.

Note that the dependence $\phi_0(\pi/2)$ on the refractive index n is characterized by two steps (at $n \approx 1.12$ and $n \approx \sqrt{2}$, see figure 2). The GO approach gives an insight into their physical meaning. One can find that the step in the region of optically soft particles is attributed to the penetration of rays with $p = 2$ into the forward hemisphere with decreasing refractive index n (see equation (7)). The step at $n \approx \sqrt{2}$ is due to the penetration of the rays with $p = 1$ into the backward hemisphere at $n > \sqrt{2}$ (see equation (18)).

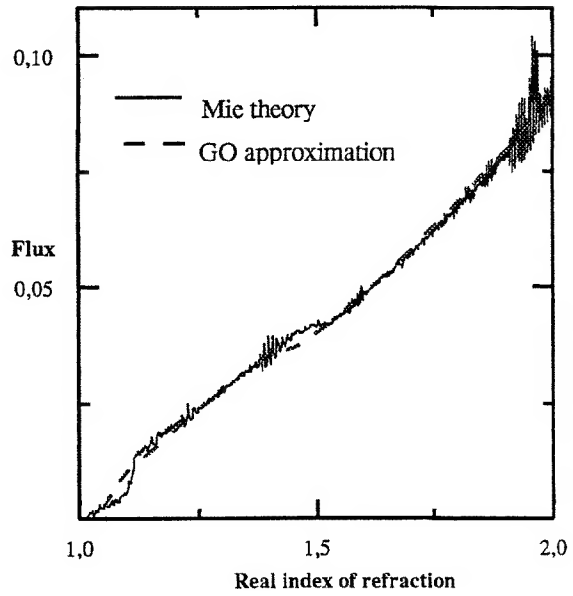

Figure 2. The flux $\phi_0(\pi/2)$ versus the particle's refractive index n (the full line shows the results of the Mie theory at $\chi = 0$ and $\rho = 10^3$; the broken line is the calculation with equations (11) and (30)).

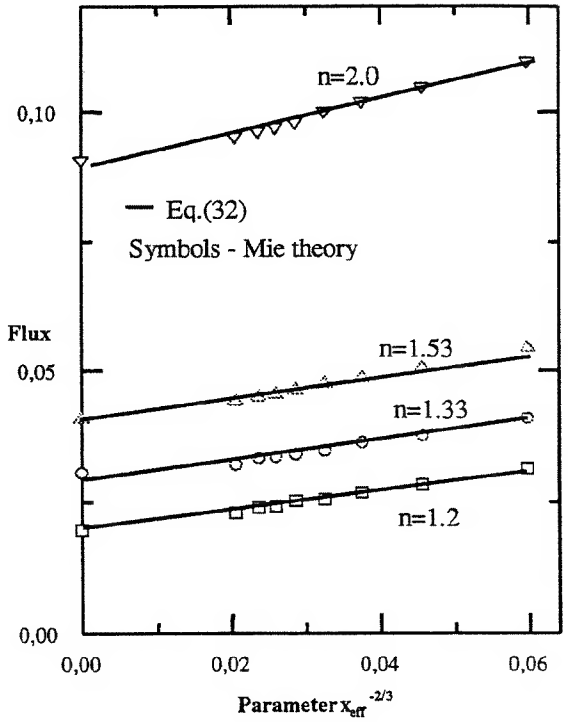

Figure 3. The flux $\phi(\pi/2)$ versus the parameter $x_{eff}^{-2/3}$ for nonabsorbing polydisperse media with the gamma PSD and various values of the refractive index n at the wavelength $\lambda = 0.55$ μm (symbols are the results of the Mie theory; full lines show the linear interpolation in accordance with equation (32)).

We found that, for $n = 1.33$ (a water aerosol in the visible range of the electromagnetic spectrum), it will suffice to take into consideration only the rays with $p = 0$ and 1 for the calculation of the backward flux $\phi_0(\pi/2)$ (see equations (16), (24) and (30) and figure 2).

3.2. Polydispersions and edge effects

The obtained GO asymptotics (see table 1) do not depend on the scatterers' size. Thus, they can be used for polydispersions of large transparent and strongly absorbing particles without any changes. This is the main reason why we choose namely cases $c = 0$ and ∞ for table 1. At intermediate values of the absorption parameter c, fluxes scattered between two angles depend on the size of particles. They vary between the values calculated at $c = 0$ and ∞ (see table 1).

The asymptotics obtained can be generalized to particles of intermediate sizes using wave corrections to the GO solution. One way to do this is to subtract the GO solutions from the Mie calculations and then to perform the parametrization of the residual [5]. In doing so, one can assume [5] that the value of $\phi(\pi/2)$ for the polydispersion of nonabsorbing particles can be described by the following relationship:

$$\phi(\pi/2) = \phi_0(\pi/2) + \frac{\alpha}{x_{eff}^{2/3}} \tag{32}$$

where $x_{eff} = 2\pi a_{eff}/\lambda$,

$$a_{eff} = \int_0^\infty a^3 f(a)\,\mathrm{d}a \Big/ \int_0^\infty a^2 f(a)\,\mathrm{d}a$$

and $f(a)$ is the particle size and distribution (PSD). At $x_{eff} \to \infty$ it follows from equation (32) that $\phi(\pi/2) \to \phi_0(\pi/2)$ (see table 1). The second term in equation (32) depends on the wavelength and represents wave corrections to the ray optics solution. As noted above, the empirical coefficient α can be evaluated by the parametrization of results obtained from the Mie theory.

Figure 3 presents the dependence of the flux $\phi(\pi/2)$ on the parameter $x_{eff}^{-2/3}$, calculated with the Mie theory ($\lambda = 0.55$ μm; $n = 1.2$, 1.33, 1.53 and 2.0; the gamma PSD $f(a) = Aa^6 \exp(-6a/a_0)$, where A is the normalization constant and $a_0 = 4$, 6, 8, 10, 12, 14, 16 and 20 μm) and with the simple equation (32). It can be seen from figure 3 that the empirical expression (32) can indeed be used to describe the backwards flux $\phi(\pi/2)$ and $\alpha \approx 0.2$ at $n = 1.2$–1.53.

4. Conclusion

We calculated here asymptotical values of light fluxes scattered by large spherical particles between two angles. Such quantities are widely used in the radiative transfer theory [1]. The results obtained can be generalized to take into account the polydispersity of disperse media. Fluxes scattered into an arbitrary angle range (for instance, from the scattering angle θ_1 (that need not be 0) to the scattering angle θ_2) can be calculated in the framework of the geometrical optics approach as well.

The value of $\phi_0(\pi/2)$ is very sensitive to the refractive index n (see, for example, the region of the first step in

figure 2) and can be used for the retrieval of the refractive index of transparent particles.

References

[1] Zege E P, Ivanov A P and Katsev I L 1991 *Image Transfer through a Scattering Medium* (Berlin: Springer)

[2] van de Hulst H C 1981 *Light Scattering by Small Particles* (New York: Dover)

[3] Shifrin K S 1951 *Scattering of Light in a Turbid Medium* (Moscow: Gostekhteorizdat)

[4] Bohren C F and Huffman D 1983 *Light Scattering and Absorption by Small Particles* (New York: Wiley)

[5] Kokhanovsky A A and Zege E 1995 *Appl. Opt.* **34** 5513

[6] Chylek P 1973 *J. Opt. Soc.* **63** 1467

[7] Wiscombe W J and Chylek P 1977 *J. Opt. Soc. Am.* **67** 572

[8] Shifrin K S 1983 *Introduction to Ocean Optics* (Leningrad: Gidrometeoizdat)

[9] Debye P 1909 *Ann. Phys. Lpz.* **30** 57–136

[10] Kokhanovsky A 1998 *Proc. 7th European Symp. on Particle Characterization Preprints* vol II, ed R Weichert (Nurnberg: Nurnberg Messe GmbH) pp 517–26